

Polyfluorinated Amino Acids for Sensitive ^{19}F NMR-Based Screening and Kinetic Measurements

Gianluca Papeo,* Patrizia Giordano, Maria Gabriella Brasca, Ferdinando Buzzo, Dannica Caronni, Franco Ciprandi, Nicola Mongelli, Marina Veronesi, Anna Vulpetti,[†] and Claudio Dalvit

Contribution from the Chemistry Department, Nerviano Medical Sciences, Viale Pasteur 10, 20014 Nerviano, Milano, Italy

Received December 20, 2006; E-mail: gianluca.papeo@nervianoms.com

Abstract: Two novel series of polyfluorinated amino acids (PFAs) were designed and synthesized according to a very short and scalable synthetic sequence. The advantages and limitations of these moieties for screening purposes are presented and discussed. The potential applications of these PFAs were tested with their incorporation into small arginine-containing peptides that represent suitable substrates for the enzyme trypsin. The enzymatic reactions were monitored by ^{19}F NMR spectroscopy, using the 3-FABS (three fluorine atoms for biochemical screening) technique. The high sensitivity achieved with these PFAs permits a reduction in substrate concentration required for 3-FABS. This is relevant in the utilization of 3-FABS in fragment-based screening for identification of small scaffolds that bind weakly to the receptor of interest. The large dispersion of ^{19}F isotropic chemical shifts allows the simultaneous measurement of the efficiency of the different substrates, thus identifying the best substrate for screening purposes. Furthermore, the knowledge of K_M and K_{cat} for the different substrates allows the identification of the structural motifs responsible for the binding affinity to the receptor and those affecting the chemical steps in enzymatic catalysis. This enables the construction of suitable pharmacophores that can be used for designing nonpeptidic inhibitors with high affinity for the enzyme or molecules that mimic the transition state. The novel PFAs can also find useful application in the FAXS (fluorine chemical shift anisotropy and exchange for screening) experiment, a ^{19}F -based competition binding assay for the detection of molecules that inhibit the interaction between two proteins.

Introduction

NMR-based screening for the identification of potential drug candidates has gained a key role in the drug discovery process.^{1,2} As more refined versions of the original techniques become available, their throughput starts to approach more conventional high-throughput screening (HTS) procedures. A number of review articles covering this topic have been recently published.^{3–16} Our long-lasting interest in exploiting ^{19}F NMR for screening

culminated with the 3-FABS (three fluorine atoms for biochemical screening) technique,¹⁷ a versatile NMR-based biochemical assay. According to this methodology, a CF_3 -tagged substrate for a given enzymatic reaction allows for the identification of inhibitors, along with accurate measurement of their IC_{50} , via ^{19}F NMR spectroscopy. This methodology was subsequently applied with success to the screening of a focused library against caspases¹⁸ and of plant extracts against HIV-1 protease¹⁹ and prolyl oligopeptidase.²⁰ However, a weak point

[†] Current address: Novartis Institute for Biomedical Research, CH-4002, Basel Switzerland.

- (1) Shuker, S. B.; Hajduk, P. J.; Meadows, R. P.; Fesik, S. W. *Science* **1996**, *274*, 1531–1534.
- (2) Hajduk, P. J.; Sheppard, D. G.; Nettlesheim, D. G.; Olejniczak, E. T.; Shuker, S. B.; Meadows, R. P.; Steinman, D. H.; Carrera, G. M., Jr.; Marcotte, P. M.; Severin, J.; Walter, K.; Smith, H.; Gubbins, E.; Simmer, R.; Holzman, T. F.; Morgan, D. W.; Davidsen, S. K.; Summers, J. B.; Fesik, S. W. *J. Am. Chem. Soc.* **1997**, *119*, 5818–5827.
- (3) (a) Moore, J. M. *Curr. Opin. Biotechnol.* **1999**, *10*, 54–58. (b) Lepre, C. A.; Moore, J. M.; Peng, J. W. *Chem. Rev.* **2004**, *104*, 3641–3675.
- (4) Hajduk, P. J.; Meadows, R. P.; Fesik, S. W. *Q. Rev. Biophys.* **1999**, *32*, 211–240.
- (5) (a) Peng, J. W.; Lepre, C. A.; Fejzo, J.; Abdul-Manan, N.; Moore, J. M. *Methods Enzymol.* **2001**, *338*, 202–230. (b) Peng, J. W.; Moore, J.; Abdul-Manan, N. *Prog. Nucl. Magn. Reson. Spectrosc.* **2004**, *44*, 225–256.
- (6) (a) Diercks, T.; Coles, M.; Kessler, H. *Curr. Opin. Chem. Biol.* **2001**, *5*, 285–291. (b) Coles, M.; Heller, M.; Kessler, H. *Drug Discovery Today* **2003**, *8*, 803–810.
- (7) (a) Pellecchia, M.; Sem, D. S.; Wüthrich, K. *Nat. Rev. Drug Discovery* **2002**, *1*, 211–219. (b) Pellecchia, M.; Becattini, B.; Crowell, K. J.; Fattorusso, R.; Forino, M.; Fragai, M.; Jung, D.; Mustelin, T.; Tautz, L. *Expert Opin. Ther. Targets* **2004**, *8*, 597–611.
- (8) Van Dongen, M.; Weigelt, J.; Uppenberg, J.; Schultz, J.; Wikström, M. *Drug Discovery Today* **2002**, *7*, 471–478.
- (9) Wyss, D. F.; McCoy, M. A.; Senior, M. M. *Curr. Opin. Drug Discovery Dev.* **2002**, *5*, 630–647.
- (10) Stockman, B. J.; Dalvit, C. *Prog. Nucl. Magn. Reson. Spectrosc.* **2002**, *41*, 187–231.
- (11) Meyer, B.; Peters, T. *Angew. Chem., Int. Ed.* **2003**, *42*, 864–890.
- (12) Zartler, E. R.; Yan, J.; Mo, H.; Kline, A. D.; Shapiro, M. J. *Curr. Top. Med. Chem.* **2003**, *3*, 25–37.
- (13) Fielding, L. *Curr. Top. Med. Chem.* **2003**, *3*, 39–53.
- (14) Salvatella, X.; Giralt, E. *Chem. Soc. Rev.* **2003**, *32*, 365–372.
- (15) (a) Jahnke, W.; Widmer, H. *Cell. Mol. Life Sci.* **2004**, *61*, 580–599. (b) Fernandez, C.; Jahnke, W. *Drug Discovery Today: Technol.* **2004**, *1*, 277–283.
- (16) Ludwiczek, M. L.; Baminger, B.; Konrat, R. *J. Am. Chem. Soc.* **2004**, *126*, 1636–1637.
- (17) (a) Dalvit, C.; Ardini, E.; Flocco, M.; Fogliatto, G. P.; Mongelli, N.; Veronesi, M. *J. Am. Chem. Soc.* **2003**, *125*, 14620–14625. (b) Dalvit, C.; Ardini, E.; Fogliatto, G. P.; Mongelli, N.; Veronesi, M. *Drug Discovery Today* **2004**, *9*, 595–602.
- (18) Fattorusso, R.; Jung, D.; Crowell, K. J.; Martino, F.; Pellecchia, M. *J. Med. Chem.* **2005**, *48*, 1649.

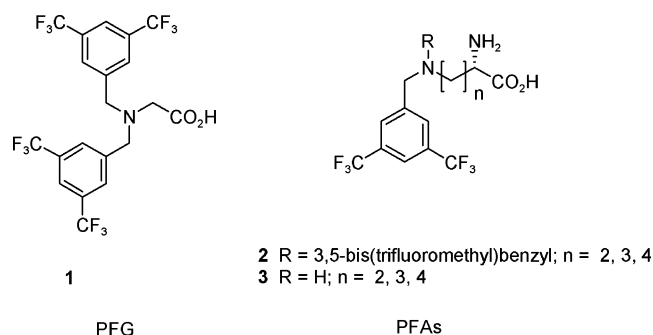
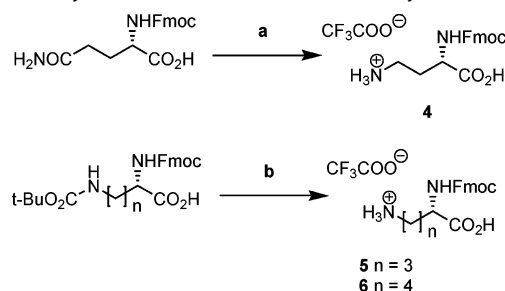


Figure 1. Chemical structures of polyfluorinated glycine (PFG) and polyfluorinated amino acids (PFAs).

of the originally formulated technique proved to be the low sensitivity compared to that of other fluorescence-based²¹ and radioactive-based²² procedures. In order to overcome this problem, two possible strategies could be envisaged: (1) use of cryogenic probe technology²³ optimized to ¹⁹F detection²⁴ and (2) use of substrates containing magnetically equivalent multiple CF₃– moieties.^{24,25} As more magnetically equivalent fluorine atoms are present in the substrate the throughput increases, less amount of enzyme is required, and weaker inhibitors can be identified. This last point is particularly relevant in a fragment-based screening approach performed with 3-FABS. Fragments are low molecular weight molecules (typically <250 Da) that display a high binding efficiency index (BEI = (–log K_D)/MW or BEI = (–log IC₅₀)/MW with MW expressed in kDa),^{26–28} but due to their small size have a weak affinity for the receptor. The detection of these weak affinity molecules can be achieved by performing the assay with a substrate concentration [S] that is comparable or smaller than its K_M (for a substrate competitive inhibitor). Recently, we synthesized PFG (polyfluorinated glycine) (**1**, Figure 1).²⁵ This unnatural amino acid has been used to cap different small arginine-containing peptides. ¹⁹F NMR studies of the trypsin-induced cleavage of the aforementioned peptides were performed at unprecedented low enzyme concentration. Increasing the distance between the cleavage site and the fluorinated moiety by systematic elongation of the peptide chain allowed us to unveil the limit of PFG **1**. This proved to be the minuscule chemical shifts difference between the signals attributed to the substrate and the product of the enzymatic reaction.

As the main drawback of PFG **1** lies on its mandatory positioning at the N-terminus of a given peptide, two novel series of polyfluorinated amino acids (PFAs) (**2**, **3**, Figure 1) engineered to be placed wherever desired along the peptide backbone were designed. 3-FABS experiments on potential trypsin

Scheme 1. Synthesis of the Intermediate Primary Amines **4–6**^a



^a Conditions and reagents: (a) [bis(trifluoroacetoxy)iodo]benzene, pyridine, DMF, H₂O, room temp, 70%; (b) DCM, TFA, room temp, quant (**5**), 98% (**6**).

substrates containing these amino acids were successfully performed. Although we have shown their application only to the 3-FABS experiments, these novel fluorinated amino acids can now find useful application also in the FAXS (fluorine chemical shift anisotropy and exchange for screening) experiment,²⁹ a ¹⁹F-based competition binding assay, for the detection in particular of molecules that inhibit the interaction between two proteins.

Results and Discussion

Synthesis of Polyfluorinated Amino Acids. N_α-Fmoc-PFAs were secured by performing a mono- or double-reductive amination reaction on the corresponding primary amines. Thus, the suitable intermediates **4–6** were prepared either by Hofmann amide degradation (**4**) from N_α-Fmoc-glutamine³⁰ or by Boc protective group removal (**5**, **6**)³¹ from N_α-Fmoc-N_δ-Boc-ornithine and N_α-Fmoc-N_ε-Boc-lysine (Scheme 1).

Reductive amination reactions performed at room temperature in a mixture of DMF/TFA 10:1 as the solvent³² employing a large excess of 3,5-bis(trifluoromethyl)benzaldehyde and sodium triacetoxyborohydride³³ (Scheme 2) delivered, after treatment with hydrochloric acid, the corresponding salts of PFAs **7–9** (Scheme 2).

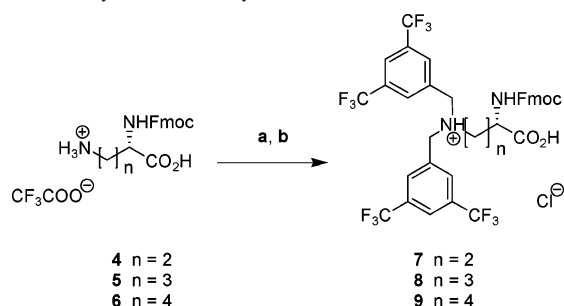
Alternatively, PFAs **10–12** were smoothly secured by performing the reductive amination reaction as before, this time in the presence of a stoichiometric amount of the fluorinated aldehyde. Compounds **10–12** were subsequently protected as their Boc derivatives **13–15** (Scheme 3).

The synthetic methodology proved to be robust and therefore scalable (a 9 g batch of compound **15** was prepared).

Synthesis of Peptides Containing Polyfluorinated Amino Acids. The subsequent synthetic campaign was then focused on the preparation of a handful of PFAs-containing peptides encompassing an arginine residue. These peptides were designed

- (19) Frutos, S.; Tarragó, T.; Giralt, E. *Bioorg. Med. Chem. Lett.* **2006**, *16*, 2677–2681.
 (20) Tarragó, T.; Frutos, S.; Rodriguez-Mias, R. A.; Giralt, E. *ChemBioChem* **2006**, *7*, 827–833.
 (21) Eggeling, C.; Brand, L.; Ullmann, D.; Jäger, S. *Drug Discovery Today* **2003**, *8*, 632–641.
 (22) Cook, N. D. *Drug Discovery Today* **1996**, *1*, 287–294.
 (23) Kovacs, H.; Moskau, D.; Spraul, M. *Prog. Nucl. Magn. Reson. Spectrosc.* **2005**, *46*, 131–155.
 (24) Dalvit, C.; Mongelli, N.; Papeo, G.; Giordano, P.; Veronesi, M.; Moskau, D.; Kümmerle, R. *J. Am. Chem. Soc.* **2005**, *127*, 13380–13385.
 (25) Dalvit, C.; Papeo, G.; Mongelli, N.; Giordano, P.; Saccardo, B.; Costa, A.; Veronesi, M.; Ko, S. Y. *Drug Dev. Res.* **2005**, *64*, 105–113.
 (26) Hopkins, A. L.; Groom, C. R.; Alex, A. *Drug Discovery Today* **2004**, *9*, 430–431.
 (27) Abad-Zapatero, C.; Metz, J. T. *Drug Discovery Today* **2005**, *10*, 464–469.
 (28) Hajduk, P. J. *J. Med. Chem.* **2006**, *49*, 6972–6976.

- (29) (a) Dalvit, C.; Flocco, M.; Veronesi, M.; Stockman, B. J. *Comb. Chem. High Throughput Screening* **2002**, *5*, 605–611. (b) Dalvit, C.; Fagerness, P. E.; Hadden, D. T. A.; Sarver, R. W.; Stockman, B. J. *J. Am. Chem. Soc.* **2003**, *125*, 7696–7703.
 (30) (a) de Macédo, P.; Marrano, C.; Keillor, J. W. *Bioorg. Med. Chem.* **2002**, *10*, 355–360. (b) Sakura, N.; Itoh, T.; Uchida, Y.; Ohki, K.; Okimura, K.; Chiba, K.; Sato, Y.; Sawanishi, H. *Bull. Chem. Soc. Jpn.* **2004**, *77*, 1915–1924.
 (31) Spectroscopic data are in agreement with those reported in the literature: (a) Varghese, J. *PCT Int. Appl.* **2003**, *204*, WO 2003045378. (b) Banwell, M. G.; McRae, K. J. *J. Org. Chem.* **2001**, *66*, 6768–6774. (c) Boyle, W. J., Jr.; Sifniades, S.; Van Peppen, J. F. *J. Org. Chem.* **1979**, *44*, 4841–4847.
 (32) Traquandi, G.; Brasca, M. G.; D'Alessio, R.; Polucci, P.; Roletto, F.; Vulpetti, A.; Pevarello, P.; Panzeri, A.; Quartieri, F.; Ferguson, R.; Vianello, P.; Fancelli, D. *PCT Int. Appl.* **2004**, *226*, WO 2004104007.
 (33) Abdel-Magid, A. F.; Maryanoff, C. A. *ACS Symp. Ser.* **1996**, *641*, 201–216.

Scheme 2. Synthesis of Polyfluorinated Amino Acids **7–9**^a

^a Conditions and reagents: (a) 9 equiv of $\text{NaBH}(\text{AcO})_3$, 6 equiv of 3,5-bis(trifluoromethyl)benzaldehyde, DMF, TFA, room temp, 3.5 h; (b) 4 N HCl, dioxane, room temp, 48% (**7**), 75% (**8**), 65% (**9**) over two steps.

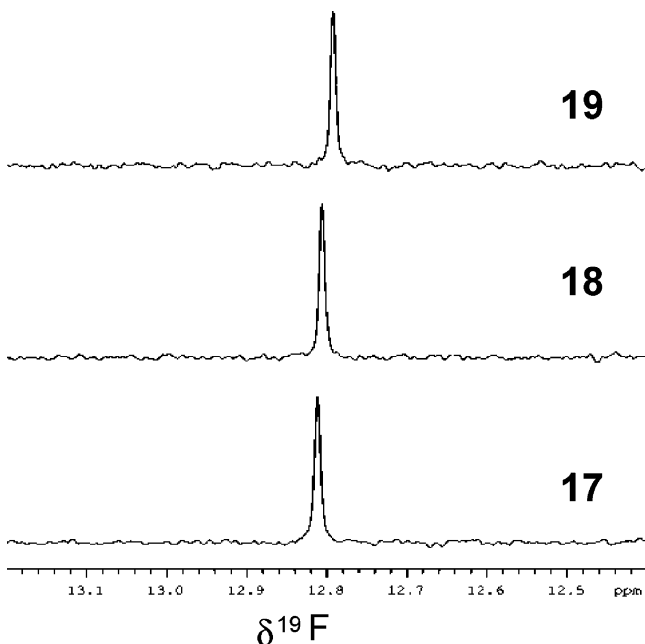


Figure 2. ^{19}F NMR spectra of the three peptides **17**, **18**, and **19** at $10\ \mu\text{M}$ concentration. The samples were in 50 mM Tris pH 7.5, 0.001% Triton X-100, and 8% D_2O for the lock signal. A total number of 64 transients were acquired for each spectrum corresponding to a 3 min recording time.

Table 1. ^{19}F Isotropic Chemical Shifts of Substrate Signals

peptide	δ_s^a	$(\delta_s - \delta_p)$ at pH 7.5 ^b	$(\delta_s - \delta_p)$ at pH 1.5 ^b
17	12.812	6.6	5.3
18	12.806	4.3	17.2
19	12.793	2.3	-3.1
20	12.904	4.7	
21	12.834	14	
22	12.785	10.1	

^a Chemical shift of substrate signal in ppm at pH 7.5. ^b Chemical shift difference of substrate and product signals in Hz.

to test PFAs as potential ^{19}F NMR tools in a trypsin-based assay. The placement of a glutamic residue at their N-termini has been deliberately chosen in order to increase the solubility of the peptides in aqueous medium. With the use of a Rink apparatus,³⁴ pentapeptides **17–22** were prepared by anchoring the growing peptide on a commercially available Rink amide AM resin^{35,36}

(34) Rink Solid Phase Washer; Rink Think Engineering; Bubendorf, Switzerland.
(35) Bernatowicz, M. S.; Daniels, S. B.; Köster, H. *Tetrahedron Lett.* **1989**, *30*, 4645–4648.

(36) Coste, J.; Le-Nguyen, D.; Castro, B. *Tetrahedron Lett.* **1990**, *31*, 205–208.

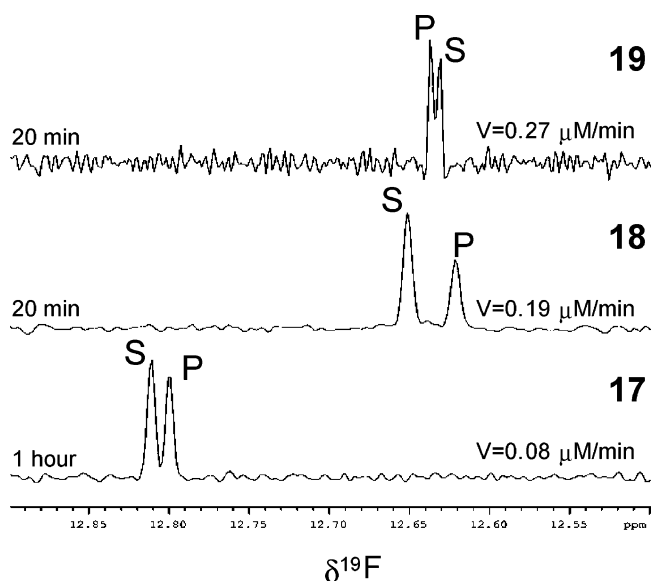


Figure 3. ^{19}F spectra of $10\ \mu\text{M}$ of peptides **17**, **18**, and **19** in the presence of 1 nM trypsin. The reaction was quenched with the addition of $80\ \mu\text{M}$ leupeptin. Spectra were acquired with 64 transients corresponding to a 3 min recording time. Samples were in 50 mM Tris, 0.001% Triton X-100, 8% D_2O for the lock signal at pH 7.5 (lower trace) and pH 1.5 (middle and upper traces). The increased noise level in the upper spectrum is due to the strong resolution enhancement ($l_b = -3$ and $g_f = 0.3$) applied to the data for resolving the two signals. S and P refer to the substrate and the cleaved substrate, respectively. The incubation time and the speed of the reaction are reported.

and exploiting well-precedented Fmoc chemistry^{37,38} (Scheme 4).

NMR Data. The ^{19}F NMR spectra of peptides **17–19** showed a single sharp and intense signal at $20\ ^\circ\text{C}$ (Figure 2). The spectra indicate the absence of additional peaks originating from conformers in slow exchange.

Fast rotation around three rotatable bonds averages the chemical shifts of the four CF_3 signals resulting in one signal originating from 12 fluorine atoms. Chemical shifts for these signals are reported in Table 1.

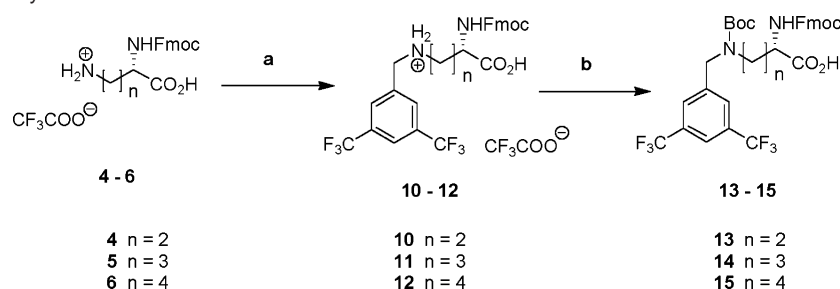
Peptides **17–19** were subsequently tested in the aforementioned trypsin-based assay, performed either at 800 pM or 1 nM enzyme concentration. All the peptides underwent the enzymatic reaction, but with different velocities (Figure 3). The velocity was obtained experimentally by measuring the integral of the ^{19}F product signal divided by the incubation time of the reaction.

The chemical shift differences for the signals of the substrate and cleaved substrate for peptides **17–19** at pH 7.5 are small, as is evident from Table 1. An improvement in the separation of the signals for peptides **18** and **19** was achieved by lowering the pH of the solution to pH 1.5, as is shown in Table 1 and Figure 3.

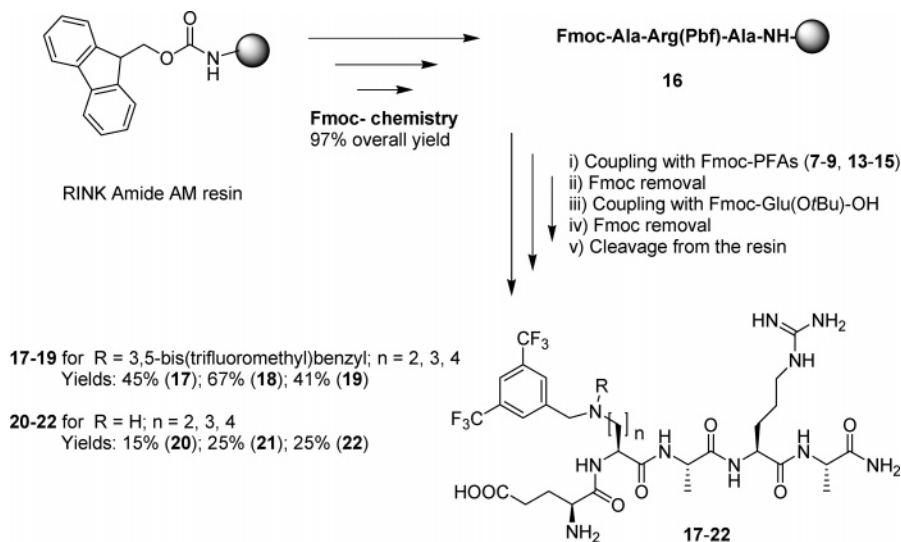
Polyfluorinated amino acids **2** have some potential drawbacks that could limit their applications. (i) The fluorinated moiety is

(37) (a) Carpino, L. A.; Han, G. Y. *J. Am. Chem. Soc.* **1970**, *92*, 5748–5749. For a review, see: (b) Fields, G. B.; Noble, R. L. *Int. J. Pept. Protein Res.* **1990**, *35*, 161–214.

(38) (a) Stewart, J.; Young, J. *Solid Phase Peptide Synthesis*; Pierce Chemical Company: Rockford, IL 1984. (b) Atherthon, E.; Sheppard, R. C. *Solid Phase Peptide Synthesis: A Practical Approach*; IRL Press: Oxford, 1989. (c) Kates, S. A.; Albericio, F., Eds. *Solid-Phase Synthesis. A Practical Guide*; Marcel Dekker: New York, 2000. (d) Chan, W. C., White, P. D., Eds. *Fmoc Solid Phase Peptide Synthesis: A Practical Approach*; Oxford University Press: Oxford, 2000.

Scheme 3. Synthesis of Polyfluorinated Amino Acids **13–15**^a

^a Conditions and reagents: (a) 3 equiv of NaBH(AcO)₃, 1.2 equiv of 3,5-bis(trifluoromethyl)benzaldehyde, DMF, TFA, room temp, 1 h, 43% (**10**), 55% (**11**), 65% (**12**); (b) (Boc)₂O, NaHCO₃(aq), AcOEt or DCM, room temp, 3 h, 83% (**13**), 98% (**14**), 98% (**15**).

Scheme 4. Synthesis of Peptides **17–22**

rather hydrophobic, and therefore, insertion of this amino acid into a peptide with low water solubility could result in a substrate with poor solubility. (ii) The large size of the PFA can interfere with the binding of the peptide to the enzyme resulting in a weak affinity substrate for the desired target. (iii) The chemical shift dispersion of the substrate and product fluorine signals tends to be small. This is due to the averaging of the chemical shift originating from rapid rotation around three bonds. The small chemical shift dispersion requires the use of high-field spectrometers or the use of shift reagents or dramatic pH changes of the medium (Figure 3). However, these two last methods are applicable only in an end-point format assay after reaction quenching, thus excluding their utilization in online kinetic measurements.

An approach for overcoming these limitations is the use of the amino acids **3**. Although they suffer from a 2-fold reduction in sensitivity when compared to the amino acids **2**, they do not have the drawbacks associated with the latter. The fluorine spectrum of the three combined substrates **20–22** (Figure 4, lower trace) displays three well-separated sharp resonances originating from the six fluorine atoms of the three substrates S_A (**20**), S_B (**21**), and S_C (**22**). Upon addition of 440 pM trypsin and after an incubation time of 260 min, three novel signals of different intensity appear in the spectrum (Figure 4, upper trace) originating from the three cleaved peptides P_A, P_B, and P_C.

All the signals of the substrates and products have different isotropic chemical shifts, and the chemical shift dispersion is significantly larger when compared to that of the peptides **17–**

19. It is also interesting to note that at pH 7.5 the ¹⁹F signals of all the products shift in the same direction similarly to what is observed with other substrates for trypsin and other proteases.^{17a,b,19} The fluorinated amino acids are at the N-terminal with respect to the cleavage site. Therefore, the observed shift for the products is probably due to the negative charge of the carboxylic

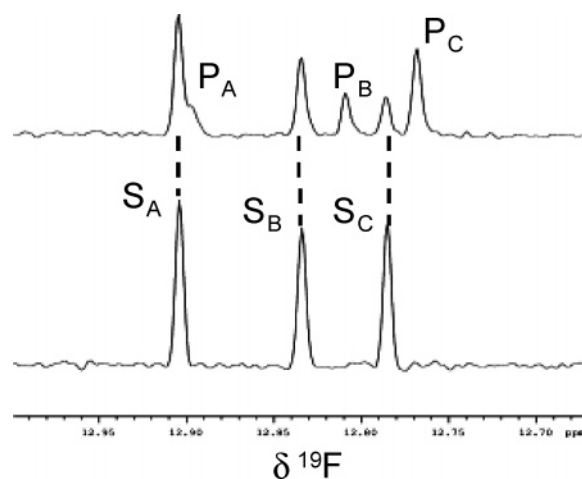


Figure 4. ¹⁹F NMR spectra of the three substrates **20–22** acquired after 4 min (lower trace) and after 260 min (upper trace) from the addition of trypsin. The concentrations of the substrates and of the enzyme were 20 μM and 440 pM, respectively. A total number of 84 transients were recorded for each spectrum corresponding to a 4 min acquisition time. The S_A, S_B, S_C, P_A, P_B, and P_C labels refer to the ¹⁹F signals of the substrates **20**, **21**, and **22** and their corresponding enzymatically cleaved peptides, respectively.

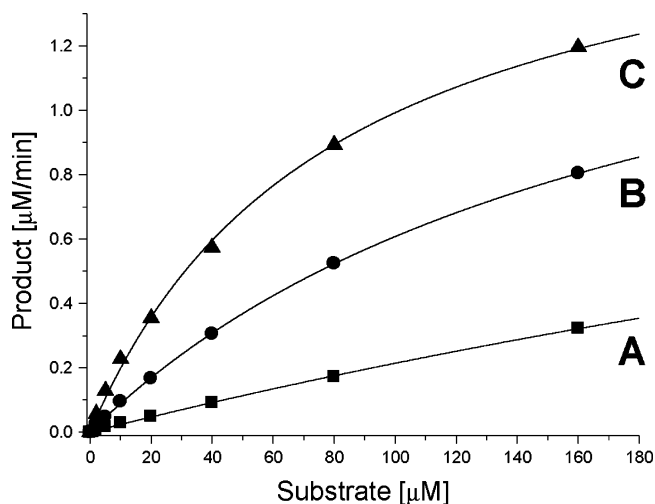


Figure 5. Plot of the enzymatic velocity (product/min) as a function of the substrate concentration. The reactions were performed in Eppendorf vials in the presence of 50 mM Tris pH 7.5, 0.001% Triton X-100, and 1 nM trypsin and quenched after a defined delay with 80 μM leupeptin. After the quenching of the reaction, the solutions were transferred to 5 mm tubes and ^{19}F spectra were recorded. Curves A, B, and C correspond to substrates S_A , S_B , and S_C , respectively. The reaction speed was calculated by dividing the normalized integral of the product ^{19}F signal (the sum of the substrate and product ^{19}F signal integrals correspond to the concentration of the peptide used in the experiments) with the incubation time. Data were analyzed with nonlinear least-squares methods in the Origin 5.0 software package. The best fit of the experimental data provides the value of K_M and K_{cat} according to the Henri–Michaelis–Menten equation.

group. The small chemical shift difference of 0.019 ppm between the ^{19}F signals of **17** and **19** is amplified to 0.119 ppm for **20** and **22**. The large chemical shift dispersion in the spectra of Figure 4 allows a direct comparison of the efficiency of the substrates. Analysis of these spectra identifies substrate S_C as the most efficient substrate with the following ranking order in efficiency: $S_C > S_B > S_A$. The possibility of monitoring simultaneously the kinetics of different substrates is important in the optimization process for the identification of the best substrate. The selected substrate can then be used in the assay or used for generating a potent inhibitor by replacing the amino acid that is modified by the enzyme. In addition, the knowledge of the K_M and K_{cat} for the different substrates allows the identification of the structural motifs responsible for the binding affinity to the receptor and those affecting the chemical steps in enzymatic catalysis. This enables the construction of a suitable pharmacophore that can be used for designing non-peptidic inhibitors with high affinity for the enzyme or molecules that mimic the transition state. The simultaneous detection of different substrates is also useful for monitoring enzymatic reaction cascades where the fluorinated product becomes the substrate of another enzyme of the cascade or where different fluorinated substrates are used in a multiple screening run.^{17b}

Titration experiments on the individual peptides as a function of the peptide concentration were performed in order to gain more detailed insight into the kinetics of these substrates and to understand the differences in catalytic enzyme efficiency. Figure 5 shows the 3-FABS results for the three peptides with the plot of the enzymatic velocity as a function of the substrate concentration.

Table 2 reports the kinetic parameters for the three peptides extracted from the experimental data shown in Figure 5.

Table 2. Kinetic Parameters for the Hydrolysis of Polyfluorinated Peptides by Trypsin at 20 °C

peptide	K_{cat} (s^{-1})	K_M (μM)	K_{cat}/K_M ($\text{s}^{-1}\text{M}^{-1}$)	$\Delta\Delta G_{\text{ES}}^\ddagger$ (kcal/mol)
20	32 ± 5	805 ± 145	0.4×10^5	
21	28 ± 2	186 ± 6	1.5×10^5	$(-0.77)^a$
22	30 ± 2	80 ± 6	3.75×10^5	$(-0.53)^b$

^{a,b} Difference in free energy between peptides **21** and **20**, **22** and **21**, respectively.

From these data it is evident that K_{cat} is the same for the three peptides, whereas K_M ranges from 80 μM for S_C to 805 μM for S_A . The identity of K_{cat} for the three peptides indicates that the chemical steps subsequent to the enzyme–substrate complex formation are not influenced by changes in size of the fluorinated amino acid. The additional binding energy originating from the added CH_2 groups is used to bind the substrate, i.e., decrease K_M . Therefore, the different catalytic enzyme efficiencies (K_{cat}/K_M) with the three substrates are simply due to their different K_M . In other words, the substrate specificity merely involves discrimination in binding of the substrates to their ground states. The ratio K_{cat}/K_M is related to the free energy difference between the free reactants (enzyme and substrate) and the transition state complex (ES^\ddagger). Table 2 reports the difference in transition state energies ($\Delta\Delta G_{\text{ES}}^\ddagger$) derived from the experimental values of K_{cat}/K_M according to the equation^{39,40}

$$\Delta\Delta G_{\text{ES}}^\ddagger = -RT \ln \frac{(K_{\text{cat}}/K_M)_{(n+2)\text{CH}_2}}{(K_{\text{cat}}/K_M)_{2\text{CH}_2}}$$

where n is 1 or 2.

The addition of the first CH_2 group results in an incremental Gibbs free energy of 0.77 kcal/mol, whereas the addition of the second CH_2 provides a supplementary smaller improvement of 0.53 kcal/mol. The same ranking order in efficiency was observed for substrates **17**–**19**. In addition, the relative magnitude changes in the initial reaction rate are also very similar with $V_{19}/V_{18} = 1.4$, $V_{22}/V_{21} = 1.6$ and $V_{19}/V_{17} = 3.3$, $V_{22}/V_{20} = 3.9$. This allows the general statement that the shorter the spacer between the fluorinated moiety and the backbone, the slower the rate of the reaction. Docking studies were performed in order to gain insight into the binding of these substrates to trypsin.

The three peptidic ligands were docked into the trypsin crystal structure (entry 2PTC in the Protein Data Bank, 1.90 Å resolution).⁴¹ The results were evaluated in term of total estimated binding energy. As expected, the arginine side chain of all the three ligands is located into the S1 binding pocket, which is occupied by a lysine in the 2PTC crystal structure. The long lysine and arginine side chains extend in the S1 pocket interacting with the carboxylic oxygens of Asp189 side chain. Through this S1 pocket interaction, trypsin favors cleavage at the amide bond next to lysine or arginine amino acids.

Figure 6 shows the top-ranked pose of ligand S_B (**21**) docked into trypsin. This proposed binding mode highlights a wide hydrogen-bonding network: between the side chain of the ligand arginine and Asp189 and between the carbonyl oxygen of the

(39) Fersht, A. *Enzyme Structure and Mechanism*; W.H. Freeman and Company: New York, 1985.

(40) Copeland, R. A. *Enzymes*; Wiley-VCH Inc.: New York, 2000.

(41) Marquart, M.; Walter, J.; Deisenhofer, J.; Bode, W.; Huber, R. *Acta Crystallogr., Sect. B* **1983**, *39*, 480–490.

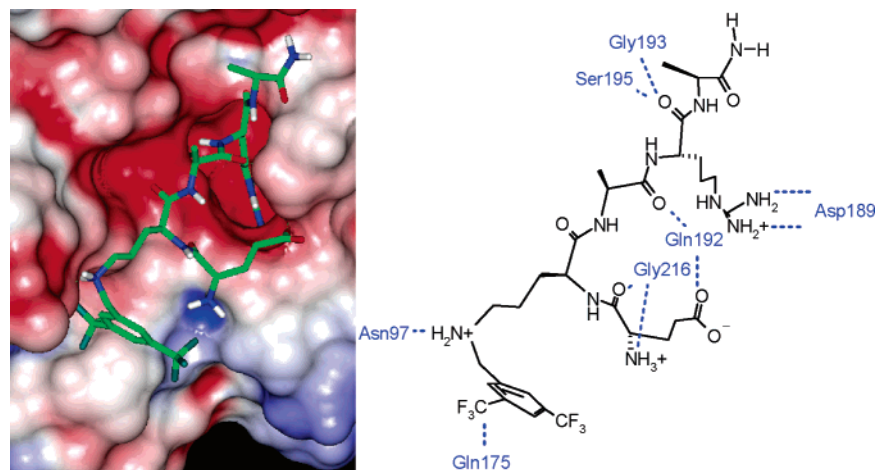


Figure 6. Best docking pose of ligand S_B (**21**) docked into trypsin. The surface is colored according to the force-field charge assigned to trypsin (left); the hydrogen-bonding interactions between trypsin and ligand are highlighted (right).

ligand arginine and Ser195 and Gly193 of trypsin. The carbonyl oxygens of the alanine and glutamic acid flanking the PFA are also involved in hydrogen bond interactions with Gln192 and Gly216 residues. One difference among the three ligands is that only ligand S_A (**20**) is not capable of making the hydrogen bond between the NH_2^+ group of the PFA and the carbonyl oxygen of the backbone of Asn97. This is due to the shorter methylenic side chains of the PFA moiety (two methylene units in ligand S_A vs three and four in ligands S_B and S_C , respectively). This might explain the lower affinity of compound S_A against trypsin.

Conclusion

In summary, we have presented the design and synthesis of novel PFAs, their insertion into short peptides, and their utilization in the 3-FABS experiments. Kinetics parameters together with the NMR properties of these different moieties have also been characterized in detail and compared. The novel amino acids can be used for tagging whichever peptide substrates wherever desired in the sequence. This results in numerous and diverse applications of the 3-FABS experiments within different drug discovery projects. In addition, their use can be extended to the FAXS-NMR-based binding assay. A short peptide that represents the amino acid sequence of a protein that is recognized by another protein can be tagged with one of these novel PFAs. The peptide is then used as a spy molecule in the FAXS experiments for the detection of inhibitors of protein–protein interactions.

Materials and Methods

1. General Considerations. Amino acid derivatives (all in their L configuration), PyBOP, and Rink amide AM resin (200–400 mesh, loading 0.68 mmol/g) were purchased from Novabiochem, Switzerland. All reagents were obtained from commercial suppliers and used as received. The abbreviations used for both the amino acids and the protecting groups are based on recommendations of the JCBN.⁴² For a complete glossary of terms see the Supporting Information.

Flash chromatography was performed on silica gel (Merck grade 9385, 60 Å). Melting points were determined in open glass capillaries with a Buchi 535 melting point apparatus and are uncorrected. Optical rotations were recorded on a Perkin-Elmer 241 polarimeter in a 1 dm cell at ambient temperature with a sodium lamp (589 nm). Exact mass

data ESI(+) were obtained on a Waters Q-ToF Ultima directly connected with an Agilent micro-HPLC 1100 as previously described.⁴³ ^1H NMR spectroscopy was performed on a Mercury VX 400 operating at 400.45 MHz equipped with a 5 mm double-resonance probe (^1H { ^{15}N – ^{31}P } ID_PFG Varian) or on an INOVA 500 operating at 499.76 MHz. ^{19}F NMR spectroscopy was performed at 20 °C on a Varian Inova 600 MHz NMR spectrometer operating at a ^{19}F Larmor frequency of 564 MHz. Full details of the HPLC/MS instrumentation and both the analytical and the purification methods used in this work can be found in the Supporting Information.

2. General Procedure for the Double-Reductive Amination Reaction. 2.1. (S)-4-[Bis-(3,5-bis-trifluoromethyl-benzyl)-amino]-2-(9H-fluoren-9-ylmethoxycarbonylamino)-butyric Acid Trifluoroacetate (7). To a solution of **4** (82 mg, 0.18 mmol) in DMF (5 mL), stirred at room temperature, sodium triacetoxyborohydride (337 mg, 1.6 mmol) and 3,5-bis(trifluoromethyl)benzaldehyde (0.18 mL, 1.08 mmol) were subsequently added. After 5 min, trifluoroacetic acid (0.5 mL) was added, and the reaction mixture was stirred at room temperature for 3.5 h. The reaction mixture was then evaporated to dryness in vacuo, taken up in dichloromethane, and the organic phase was washed with water and brine, dried over Na_2SO_4 , and concentrated. The crude material was then purified by flash chromatography (cyclohexane/AcOEt 50/50, AcOEt, and then AcOEt/MeOH 80/20) to afford compound **7** (100 mg, 61% yield) as a white solid: mp 152 °C, $[\alpha]_D +1.2$ (c 1, MeOH). ^1H NMR (400 MHz, $\text{DMSO}-d_6$): δ ppm 7.73–7.92 (m, 8 H), 7.65 (d, $J = 7.93$ Hz, 2 H), 7.25–7.46 (m, 4 H), 6.91 (s, 1 H), 4.12–4.32 (m, 3 H), 3.69–3.95 (m, 5 H), 2.73 (t, $J = 6.58$ Hz, 2 H), 1.82–2.14 (m, 2 H). HRMS (ES+): m/z calcd for $\text{C}_{37}\text{H}_{29}\text{F}_{12}\text{N}_2\text{O}_4$, 793.1930 $[\text{M} + \text{H}]^+$; found, 793.1957. ^{19}F NMR ($\text{DMSO}-d_6$): 11.84 ppm.

2.2. (S)-5-[Bis-(3,5-bis-trifluoromethyl-benzyl)-amino]-2-(9H-fluoren-9-ylmethoxycarbonylamino)-pentanoic Acid Trifluoroacetate (8). With the use of the procedure described above, starting from **5** (125 mg, 0.27 mmol), compound **8** was obtained (151 mg, 61% yield) as a white solid: mp 141 °C, $[\alpha]_D +3.0$ (c 1, MeOH). ^1H NMR (400 MHz, $\text{DMSO}-d_6$): δ ppm 7.77–7.93 (m, 8 H), 7.65 (d, $J = 7.68$ Hz, 2 H), 7.35–7.42 (m, 2 H), 7.24–7.33 (m, 2 H), 6.77–7.08 (br s, 1 H), 4.14–4.34 (m, 3 H), 3.70–3.87 (m, 5 H), 2.62 (t, $J = 6.43$ Hz, 2 H), 1.73–1.86 (m, 1 H), 1.47–1.72 (m, 3 H). HRMS (ES+): m/z calcd for $\text{C}_{38}\text{H}_{31}\text{F}_{12}\text{N}_2\text{O}_4$, 807.2087 $[\text{M} + \text{H}]^+$; found, 807.2093. ^{19}F NMR ($\text{DMSO}-d_6$): 11.83 ppm.

2.3. (S)-6-[Bis-(3,5-bis-trifluoromethyl-benzyl)-amino]-2-(9H-fluoren-9-ylmethoxycarbonylamino)-hexanoic Acid Trifluoroacetate (9). With the use of the procedure described above, starting from **6** (128

(42) IUPAC-IUB Joint Commission on Biochemical Nomenclature (JCBN). *Eur. J. Biochem.* **1984**, *138*, 9–37.

(43) Colombo, M.; Riccardi-Sirtori, F.; Rizzo, V. *Rapid Commun. Mass Spectrom.* **2004**, *18*, 511–517.

mg, 0.27 mmol), compound **9** was obtained (152 mg, 60% yield) as a white solid: mp 121 °C, [α]_D −2.3 (c 1, MeOH). ¹H NMR (400 MHz, DMSO-*d*₆): δ ppm 7.78–7.9 (m, 8 H), 7.62 (d, *J* = 7.72 Hz, 2 H), 7.32–7.38 (t, *J* = 6.22 Hz, 2 H), 7.22–7.3 (t, *J* = 6.54 Hz, 2 H), 6.62–6.72 (br s, 1 H), 4.15–4.23 (m, 3 H), 3.65–3.78 (m, 5 H), 2.58 (t, 2 H), 1.62–1.78 (m, 1 H), 1.43–1.58 (m, 3 H), 1.19–1.3 (m, 2 H). HRMS (ES⁺): *m/z* calcd for C₃₉H₃₃F₁₂N₂O₄, 821.2243 [M + H]⁺; found, 821.2273. ¹⁹F NMR (DMSO-*d*₆): 11.83 ppm.

3. Procedure for the Conversion of Compounds 7–9 into Their Corresponding Hydrochloride Salts. Pure TFA salts **7–9** were dissolved in dry dioxane (1 mmol in 16 mL) and exposed to a 4 N solution of hydrochloric acid in dioxane (4 mL). The resulting solutions were stirred at room temperature for 1 h and then evaporated to dryness. The corresponding hydrochloride salts were subsequently used without any further purification.

4. General Procedure for the Monoreductive Amination Reaction. 4.1. (S)-4-(3,5-Bis-trifluoromethyl-benzylamino)-2-(9H-fluoren-9-ylmethoxycarbonylamino)-butyric Acid Trifluoroacetate (10). To a solution of **4** (177 mg, 0.39 mmol) in DMF (5 mL), stirred at room temperature, sodium triacetoxyborohydride (290 mg, 1.4 mmol) and 3,5-bis(trifluoromethyl)benzaldehyde (0.07 mL, 0.43 mmol) were subsequently added. After 20 min, TFA (0.5 mL) was added, and the reaction mixture was stirred at room temperature for 1 h. The reaction mixture was then poured into water (20 mL), and the pH was adjusted to 6–7, using aqueous NaOH 32% w/w. The aqueous phase was then extracted with AcOEt (2 × 20 mL). The combined organic phases were washed with water (3 × 50 mL) and brine, dried over Na₂SO₄, and evaporated to dryness. The crude material was finally purified by flash chromatography (dichloromethane, dichloromethane/MeOH 95/5, dichloromethane/MeOH 80/20) to afford compound **10** as a white solid (114 mg, 43% yield): mp > 158 °C (decomposition), [α]_D +1.1 (c 1, MeOH). ¹H NMR (400 MHz, DMSO-*d*₆): δ ppm 8.09 (s, 2 H), 7.99 (s, 1 H), 7.89 (d, *J* = 7.44 Hz, 2 H), 7.69 (d, *J* = 7.93 Hz, 2 H), 7.42 (t, *J* = 7.32 Hz, 2 H), 7.24–7.37 (m, 3 H), 4.13–4.37 (m, 3 H), 3.88–4.08 (m, 3 H), 2.61–2.79 (m, 2 H), 1.85–2.00 (m, 1 H), 1.72–1.85 (m, 1 H). HRMS (ES⁺): *m/z* calcd for C₂₈H₂₅F₆N₂O₄, 567.1713 [M + H]⁺; found, 567.1693. ¹⁹F NMR (DMSO-*d*₆): mixture of rotational isomers; 12.15 ppm (major), 12.02 ppm (minor). ¹⁹F NMR (50 mM Tris, 1 mM DTT, 0.001% Triton X-100, pH = 7.5): mixture of rotational isomers; 12.83 ppm (major), 12.81 ppm (minor).

4.2. (S)-5-(3,5-Bis-trifluoromethyl-benzylamino)-2-(9H-fluoren-9-ylmethoxycarbonylamino)-pentanoic Acid Trifluoroacetate (11). With the use of the procedure described above, starting from **5** (2.2 g, 4.7 mmol), compound **11** was obtained (1.8 g, 55% yield) as a white solid: mp 162 °C, [α]_D +7.3 (c 1, MeOH). ¹H NMR (400 MHz, DMSO-*d*₆): δ ppm 8.06 (s, 2 H), 7.96 (s, 1 H), 7.89 (d, *J* = 7.44 Hz, 2 H), 7.71 (d, *J* = 7.44 Hz, 2 H), 7.42 (t, *J* = 7.44 Hz, 2 H), 7.27–7.37 (m, 3 H), 4.19–4.33 (m, 3 H), 3.84–3.94 (m, 3 H), 2.52–2.58 (m, 2 H), 1.73–1.83 (m, 1 H), 1.59–1.71 (m, 1 H), 1.48–1.59 (m, 2 H). HRMS (ES⁺): *m/z* calcd for C₂₉H₂₇F₆N₂O₄, 581.1870 [M + H]⁺; found, 581.1875. ¹⁹F NMR (50 mM Tris, 1 mM DTT, 0.001% Triton X-100, pH = 7.5): 12.78 ppm.

4.3. (S)-6-(3,5-Bis-trifluoromethyl-benzylamino)-2-(9H-fluoren-9-ylmethoxycarbonylamino)-hexanoic Acid Trifluoroacetate (12). With the use of the procedure described above, starting from **6** (2.8 g, 5.81 mmol), compound **12** was obtained (2.23 g, 54% yield) as a white solid: mp > 160 °C (decomposition). ¹H NMR (400 MHz, DMSO-*d*₆): δ ppm 8.04 (s, 2 H), 7.94 (s, 1 H), 7.89 (d, *J* = 7.44 Hz, 2 H), 7.69 (d, *J* = 6.95 Hz, 2 H), 7.43 (t, *J* = 7.44 Hz, 2 H), 7.28–7.38 (m, 3 H), 4.17–4.33 (m, 3 H), 3.73–3.93 (m, 3 H), 2.43–2.52 (m, 2 H), 1.65–1.79 (m, 1 H), 1.51–1.63 (m, 1 H), 1.28–1.49 (m, 4 H). HRMS (ES⁺): *m/z* calcd for C₃₀H₂₉F₆N₂O₄, 595.2026 [M + H]⁺; found, 595.2047. ¹⁹F NMR (50 mM Tris, 1 mM DTT, 0.001% Triton X-100, pH = 7.5): 12.76 ppm.

5. General Procedure for the Introduction of the *t*-Butoxycarbonyl Protective Group. 5.1. (S)-4-[(3,5-Bis-trifluoromethyl-benzyl)-

***tert*-butoxycarbonyl-amino]-2-(9H-fluoren-9-ylmethoxycarbonyl-amino)-butyric Acid (13).** To a stirred solution of compound **10** (200 mg, 0.29 mmol) in AcOEt (2 mL), saturated aqueous NaHCO₃ (2 mL) and di-*tert*-butyl dicarbonate (256 mg, 1.18 mmol) were added. The biphasic system was swirled for 3 h at room temperature. The reaction mixture was diluted with additional AcOEt; the organic phase was separated, washed with water and then with brine. Finally, it was dried over Na₂SO₄ and evaporated to dryness. The crude material was purified by flash chromatography (dichloromethane, dichloromethane/MeOH 95/5, dichloromethane/MeOH 90/10) to afford compound **13** (160 mg, 83% yield) as a white foam: mp 178 °C, [α]_D +5.8 (c 1, MeOH). ¹H NMR (400 MHz, DMSO-*d*₆): δ ppm 8.01 (s, 1 H), 7.81–7.94 (m, 4 H), 7.68 (d, *J* = 7.80 Hz, 2 H), 7.41 (t, *J* = 7.44 Hz, 2 H), 7.23–7.35 (m, 3 H), 4.54 (br s, 2 H), 4.17–4.33 (m, 3 H), 3.74 (br s, 1 H), 3.32–3.45 (m, 2 H), 1.91–2.05 (m, 1 H), 1.73–1.85 (m, 1 H), 1.28–1.45 (br s, 9 H). HRMS (ES⁺): *m/z* calcd for C₃₃H₃₃F₆N₂O₆, 667.2237 [M + H]⁺; found, 667.2266. ¹⁹F NMR (50 mM Tris, 1 mM DTT, 0.001% Triton X-100, pH = 7.5): mixture of rotational isomers; 12.88 ppm (major), 12.83 ppm (minor).

5.2. (S)-5-[(3,5-Bis-trifluoromethyl-benzyl)-*tert*-butoxycarbonyl-amino]-2-(9H-fluoren-9-ylmethoxycarbonylamino)-pentanoic Acid (14). With the use of the procedure described above, starting from **11** (195 mg, 0.28 mmol), and using dichloromethane (2 mL) instead of AcOEt, compound **14** was obtained (195 mg, 98% yield) as a white foam: mp > 170 °C (decomposition), [α]_D +5.0 (c 1, MeOH). ¹H NMR (400 MHz, DMSO-*d*₆): δ ppm 8.00 (s, 1 H), 7.84–7.94 (m, 4 H), 7.69 (d, *J* = 7.56 Hz, 2 H), 7.42 (t, *J* = 7.28 Hz, 2 H), 7.27–7.37 (m, 3 H), 7.06 (br s, 1 H), 4.51 (br s, 2 H), 4.16–4.32 (m, 3 H), 3.78 (br s, 1 H), 3.17–3.33 (m, 2 H), 1.65–1.75 (m, 1 H), 1.48–1.62 (m, 3 H), 1.19–1.48 (br s, 9 H). HRMS (ES⁺): *m/z* calcd for C₃₄H₃₅F₆N₂O₆, 681.2394 [M + H]⁺; found, 681.2425. ¹⁹F NMR (50 mM Tris, 1 mM DTT, 0.001% Triton X-100, pH = 7.5): 12.83 ppm.

5.3. (S)-6-[(3,5-Bis-trifluoromethyl-benzyl)-*tert*-butoxycarbonyl-amino]-2-(9H-fluoren-9-ylmethoxycarbonylamino)-hexanoic Acid (15). With the use of the procedure described above, starting from **12** (200 mg, 0.29 mmol), and using dichloromethane (2 mL) instead of AcOEt, compound **15** was obtained (185 mg, 98% yield) as a white foam: mp 68 °C, [α]_D −4.1 (c 1, MeOH). ¹H NMR (400 MHz, DMSO-*d*₆): δ ppm 8.02 (s, 1 H), 7.84–7.95 (m, 4 H), 7.72 (d, *J* = 7.44 Hz, 2 H), 7.59 (d, *J* = 8.41 Hz, 1 H), 7.42 (t, *J* = 7.44 Hz, 2 H), 7.33 (d, *J* = 7.56 Hz, 2 H), 7.10 (br s, 1 H), 4.48–4.60 (m, 2 H), 4.17–4.36 (m, 3 H), 3.85–3.98 (m, 1 H), 3.14–3.28 (m, 2 H), 1.22–1.75 (m, 15 H). HRMS (ES⁺): *m/z* calcd for C₃₅H₃₇F₆N₂O₆, 695.2550 [M + H]⁺; found, 695.2574. ¹⁹F NMR (50 mM Tris, 1 mM DTT, 0.001% Triton X-100, pH = 7.5): 12.84 ppm.

6. General Procedure for the Solid-Phase Peptide Synthesis. The peptide synthesis was performed on the solid phase starting from the commercially available Rink amide AM resin, 4-(2',4'-dimethoxyphenyl-Fmoc-aminomethyl)-phenoxyacetamido-norleucyl-aminomethyl copoly(styrene-1% DVB). The resin was always preswelled with DCM and DMA and accurately washed with DMA, NMP, and 2-propanol after coupling, capping, and deprotection steps.

The synthesis of the supported tripeptide **16**, Fmoc-Ala-Arg(Pbf)-Ala-NH-Rink amide AM resin, was exploited on a Rink apparatus.³⁴ The Fmoc deprotection was achieved with rapid (1 min) and multiple (usually 14–15) treatments with the mixture of piperidine/DMA 20%. For each elongation step a double coupling occurred (60 and 120 min, respectively), using each time 2 equiv of the appropriate amino acid, 2 equiv of PyBOP, and 10–12 equiv of DIEA (Hunig's base), in DMA as solvent. A capping step usually followed: two 5–10 min reactions with the mixture DMA/Ac₂O/DIEA 80:15:5. After thorough drying, 4.05 g of peptide **16** was obtained (97% yield based on resin loading).

Six samples of **16**, 160 mg each, were then transferred into a Quest 210 synthesizer⁴⁴ for further elongation with the PFAs **7–9**, **13–15**

(44) Quest 210; Argonaut Technologies: Foster City, CA.

and the Fmoc-Glu(OtBu)-OH. Double-coupling and capping steps were exploited as described before, while the alternate Fmoc-deprotection steps were performed with piperidine/DMA 20%, three times for 1, 5, and 20 min, respectively. The six Fmoc-deprotected peptides were finally cleaved from the resin as C-terminal amides by treatment with a mixture of TFA/TIS/H₂O 95/2.5/2.5,⁴⁵ repeated twice for 60 and 30 min, respectively. After filtration, the resins were washed three times with DCM, and the collected solutions were evaporated to dryness. The desired crude pentapeptides **17–22** were obtained as yellowish solids by trituration with ether and afterward submitted to HPLC purification as extensively described in the Supporting Information.

6.1. H-Glu-X_{1aa}-Ala-Arg-Ala-NH₂ Trifluoroacetate (17). Where X_{1aa} is compound **2** with $n = 2$. Overall yield: 45%. Retention time: 9.869 min. MW (monoisotopic) calcd for C₃₉H₄₈F₁₂N₁₀O₇: 996.35. MS (ES+): 998.34 [M + H]⁺, 500.02 [M + 2H]²⁺/2. MS (ES-): 996.37 [M - H]⁻. ¹⁹F NMR (50 mM Tris, 1 mM DTT, 0.001% Triton X-100, pH = 7.5): 12.81 ppm.

6.2. H-Glu-X_{2aa}-Ala-Arg-Ala-NH₂ Trifluoroacetate (18). Where X_{2aa} is compound **2** with $n = 3$. Overall yield: 67%. Retention time: 9.474 min. MW (monoisotopic) calcd for C₄₀H₅₀F₁₂N₁₀O₇: 1010.37. MS (ES+): 1012.36 [M + H]⁺, 507.00 [M + 2H]²⁺/2. ¹⁹F NMR (50 mM Tris, 1 mM DTT, 0.001% Triton X-100, pH = 7.5): 12.80 ppm.

6.3. H-Glu-X_{3aa}-Ala-Arg-Ala-NH₂ Trifluoroacetate (19). Where X_{3aa} is compound **2** with $n = 4$. Overall yield: 41%. Retention time: 9.503 min. MW (monoisotopic) calcd for C₄₁H₅₂F₁₂N₁₀O₇: 1024.38. MS (ES+): 1026.45 [M + H]⁺, 514.06 [M + 2H]²⁺/2. MS (ES-): 1024.46 [M - H]⁻. ¹⁹F NMR (50 mM Tris, 1 mM DTT, 0.001% Triton X-100, pH = 7.5): 12.79 ppm.

6.4. H-Glu-X_{4aa}-Ala-Arg-Ala-NH₂ (20). Where X_{4aa} is compound **3** with $n = 2$. Overall yield: 15%. Retention time: 0.876 min. MW (monoisotopic) calcd for C₃₀H₄₄F₆N₁₀O₇: 770.33. MS (ES+): 771.19 [M + H]⁺, 386.17 [M + 2H]²⁺/2. MS (ES-): 769.28 [M - H]⁻. ¹⁹F NMR (50 mM Tris, 1 mM DTT, 0.001% Triton X-100, pH = 7.5): 12.90 ppm.

6.5. H-Glu-X_{5aa}-Ala-Arg-Ala-NH₂ (21). Where X_{5aa} is compound **3** with $n = 3$. Overall yield: 25%. Retention time: 0.909 min. MW (monoisotopic) calcd for C₃₁H₄₆F₆N₁₀O₇: 784.35. MS (ES+): 785.24 [M + H]⁺, 393.17 [M + 2H]²⁺/2. MS (ES-): 783.35 [M - H]⁻. ¹⁹F NMR (50 mM Tris, 1 mM DTT, 0.001% Triton X-100, pH = 7.5): 12.83 ppm.

6.6. H-Glu-X_{6aa}-Ala-Arg-Ala-NH₂ (22). Where X_{6aa} is compound **3** with $n = 4$. Overall yield: 25%. Retention time: 0.95 min. MW

(monoisotopic) calcd for C₃₂H₄₈F₆N₁₀O₇: 798.36. MS (ES+): 799.26 [M + H]⁺, 400.17 [M + 2H]²⁺/2. MS (ES-): 797.33 [M - H]⁻. ¹⁹F NMR (50 mM Tris, 1 mM DTT, 0.001% Triton X-100, pH = 7.5): 12.78 ppm.

7. NMR. The enzyme trypsin and the inhibitor leupeptin were purchased from Roche Molecular Biochemical (cat. nos. 1418475 and 1017101, respectively). The enzymatic reactions were performed at room temperature in 50 mM Tris pH 7.5, 0.001% Triton X-100, and 8% D₂O for the lock signal. The concentration of substrates was 10 and 20 μM for **17–19** and **20–22**, respectively. Reactions were quenched after a defined delay with the addition of 80 μM leupeptin.

All NMR spectra were recorded at 20 °C with a Varian Inova 600 MHz NMR spectrometer operating at a ¹⁹F Larmor frequency of 564 MHz. A 5 mm probe with the inner coil tunable to either ¹⁹F or ¹H frequency was used. The instrument was equipped with a sample management system (SMS) autosampler for automatic data collection. The data were recorded without proton decoupling with an acquisition time of 0.8 s and a relaxation delay of 2.8 s. Chemical shifts are referenced to trifluoroacetic acid.

8. Docking Studies. The bound inhibitor present in the crystal structure (entry 2PTC in the Protein Data Bank, 1.90 Å resolution) was removed as well as all water molecules except one, buried deep in the S1 pocket (corresponding to HOH-416). Polar hydrogens were added to the protein, the lysine and arginine residues were positively charged, the glutamic and aspartic acid residues were negatively charged, while the histidines were defined as neutral. The docking studies were performed with the program QXP,⁴⁶ using the docking algorithm, referred to as MCDock. During the docking the protein was kept rigid; the HOH-416 water oxygen was instead treated as partially flexible, while its hydrogens were treated as completely flexible. The three peptidic ligands were docked as completely flexible. The docking runs included 10 000 steps of Monte Carlo perturbation and final energy minimization.

Acknowledgment. This work was supported by the Italian Grant FIRB RBNE03LF7X of the Ministero dell'Istruzione, dell'Università e della Ricerca.

Supporting Information Available: Glossary, HPLC/MS instrumentation, and methods. This material is available free of charge via the Internet at <http://pubs.acs.org>.

JA069128S

(45) Pearson, D. A.; Mary Blanchette, M.; Baker, M. L.; Guindon, C. A. *Tetrahedron Lett.* **1989**, *30*, 2739–2742.

(46) McMartin, C.; Bohacek, R. S. *J. Comput.-Aided Mol. Des.* **1997**, *11*, 333–344.